PUBLISHED VERSION

Kasra Sabermanesh, Luke R. Holtham, Jessey George, Ute Roessner, Berin A. Boughton, Sigrid Heuer, Mark Tester, Darren C. Plett and Trevor P. Garnett
Transition from a maternal to external nitrogen source in maize seedlings
Journal of Integrative Plant Biology, 2017; 59(4):261-274

Originally published at:
http://doi.org/10.1111/jipb.12525

JIPB Journal of Integrative Plant Biology

Transition from a maternal to external nitrogen source in maize seedlings[OO]

Kasra Sabermanesh[1,2], Luke R. Holtham[1,2], Jessey George[1,2], Ute Roessner[3,4], Berin A. Boughton[4], Sigrid Heuer[1,2], Mark Tester[1,5], Darren C. Plett[1,2] and Trevor P. Garnett[1,2,6]

1. Australian Centre for Plant Functional Genomics, Waite Research Institute, University of Adelaide, Adelaide, SA 5064, Australia
2. School of Agriculture, Food and Wine, Waite Research Institute, University of Adelaide, Adelaide, SA 5064, Australia
3. Australian Centre for Plant Functional Genomics, School of BioSciences, University of Melbourne, Parkville, Vic. 3010, Australia
4. Metabolomics Australia, School of BioSciences, University of Melbourne, Vic. 3010, Australia
5. King Abdullah University of Science and Technology, Center for Desert Agriculture, Thuwal 23955-6900, Kingdom of Saudi Arabia
6. The Australian Plant Phenomics Facility, The Plant Accelerator, Waite Campus, The University of Adelaide, Adelaide, SA 5064, Australia
*Correspondence: Darren C. Plett (darren.plett@acpfg.com.au)
doi: 10.1111/jipb.12525

Research Article

Abstract Maximizing NO_3^- uptake during seedling development is important as it has a major influence on plant growth and yield. However, little is known about the processes leading to, and involved in, the initiation of root NO_3^- uptake capacity in developing seedlings. This study examines the physiological processes involved in root NO_3^- uptake and metabolism, to gain an understanding of how the NO_3^- uptake system responds to meet demand as maize seedlings transition from seed N use to external N capture. The concentrations of seed-derived free amino acids within root and shoot tissues are initially high, but decrease rapidly until stabilizing eight days after imbibition (DAI). Similarly, shoot N% decreases, but does not stabilize until 12–13 DAI. Following the decrease in free amino acid concentrations, root NO_3^- uptake capacity increases until shoot N% stabilizes. The increase in root NO_3^- uptake capacity corresponds with a rapid rise in transcript levels of putative NO_3^- transporters, *ZmNRT2.1* and *ZmNRT2.2*. The processes underlying the increase in root NO_3^- uptake capacity to meet N demand provide an insight into the processes controlling N uptake.

Edited by: Miguel A. Piñeros, USDA-ARS, Cornell University, USA
Received Nov. 28, 2016; **Accepted** Jan. 4, 2017; **Online on** Feb. 7, 2017
OO: OnlineOpen, paid by authors

OnlineOpen

INTRODUCTION

Currently over 100 Mt of nitrogen (N) fertilizers are applied to crops each year, globally, to maximize growth and ultimately, yield, of which around 60% is applied to cereals (Heffer 2013). On average, however, cereal crops capture only 40%–50% of the applied N (Peoples et al. 1995; Sylvester-Bradley and Kindred 2009), with the remainder lost by leaching into groundwater, in surface run-off and volatilization into the atmosphere, all of which impacts considerably on the environment (Vitousek et al. 1997). Improvements in this low N uptake efficiency could greatly reduce the economic and environmental impacts attributable to

Abbreviations

DAI	days after imbibition
DW	dry weight
HATS	high affinity nitrate transport system
LATS	low-affinity nitrate transport system
N	nitrogen
NO_3^-	nitrate
NR	nitrate reductase
NRT	nitrate transporter
RN	root nitrogen
ShN	shoot nitrogen
SN	seed nitrogen

loss of N. One possible means to improve N uptake efficiency is to enhance a plant's capacity to take up nitrate (NO_3^-), as this is the predominant form of N available to plants in most agricultural soils (Wolt 1994; Miller et al. 2007).

Plant NO_3^- uptake is mediated by low-affinity (LATS) and high-affinity (HATS) transport systems, which are thought to operate predominately at high or low external NO_3^- concentrations, respectively (Glass and Siddiqi 1995; Glass 2003; Glass and Kotur 2013). In *Arabidopsis*, the NO_3^- transporters (NRTs, now named NPFs (Léran et al. 2014) AtNPF6.3/NRT1.1 and AtNRT1.2/NPF4.6 have been associated with LATS NO_3^- uptake (Huang et al. 1999). However, studies have shown that AtNPF6.3 is a unique NO_3^- transporter, as it has the capacity to mediate both low- and high-affinity NO_3^- uptake, subject to its phosphorylation state (Ho et al. 2009; Parker and Newstead 2014). However, AtNPF6.3 only plays a very minor contribution to HATS NO_3^- uptake (Glass and Kotur 2013). Conversely, AtNRT2.1 and AtNRT2.2 mediate HATS NO_3^- uptake; AtNRT2.1 is thought to be responsible for the majority of HATS activity, while AtNRT2.2 makes a smaller contribution (Li et al. 2007). Although the role of NRT2.5 remains to be clarified, it is suggested that this transporter facilitates root HATS NO_3^- uptake and re-mobilization in N-starved *Arabidopsis* (Lezhneva et al. 2014). Studies in oilseed rape and maize suggest that, compared to the LATS, the HATS is responsible for much of the NO_3^- uptake, even at NO_3^- concentrations >1 mM, and is also the system that responds to N supply and demand (Malagoli et al. 2004; Garnett et al. 2013).

Studies in *Arabidopsis* have shown that, following a NO_3^- starvation period, HATS activity and transcript levels of *AtNRT2.1* and *AtNRT2.2* increase quickly with NO_3^- resupply, but are later repressed with prolonged exposure to sufficient NO_3^- (Zhuo et al. 1999; Okamoto et al. 2003). Although NO_3^- resupply stimulates NO_3^- uptake capacity, the internal accumulation of NO_3^- and its assimilatory products, such as amino acids, repress *NRT2* transcription (Zhuo et al. 1999; Vidmar et al. 2000) and NO_3^- uptake capacity (Muller and Touraine 1992; Tischner 2000). Such observations suggest that a mechanism exists to coordinate NO_3^- uptake with plant N demand (Forde 2002). However, in most of these studies, the free N-metabolite of interest was applied exogenously, making it difficult to distinguish between the internal and external effects of these substrates.

Soon after seed imbibition, the N requirements of developing seedlings are met by the hydrolysis of finite seed protein reserves that are then transported into developing coleoptile and roots (Harvey and Oaks 1974; Watt and Cresswell 1987). When this protein reserve is exhausted, seedlings must make the transition to external N capture, in order to meet N demand and to maintain growth. This transition provides an ideal system to dissect the regulation of root NO_3^- uptake capacity.

The objective of this study was to improve our understanding of the way that cereals upregulate their NO_3^- uptake system in order to meet N demand. To this end, high temporal resolution was used between 3–15 d after imbibition (DAI), in an investigation of the root processes involved in increasing NO_3^- uptake and metabolism across the transition from seed N use to external N capture.

RESULTS

Seedling growth

On the final sampling day (21 DAI), seedlings grown in low (0.5 mM) NO_3^- had produced 18% less shoot dry matter than those in the sufficient NO_3^- treatment (2.5 mM) (Figure 1A). External NO_3^- supply had no effect on root dry weight (DW) (Figure 1B). Root:shoot ratio was followed throughout seedling development, as changes to biomass allocation, relative to nutrient supply, signify that demand is exceeding supply (Chapin et al. 1987; Ingestad and Agren 1991). During early growth (6–8 DAI), the root:shoot decreased by half for both NO_3^- treatments (Figure 1C). Following this, the root:shoot increased, and this ratio increased further in plants grown with 0.5 mM NO_3^- compared to those in 2.5 mM NO_3^-. Nitrate treatment differences in root:shoot emerged at 12 DAI and carried through to the final harvest.

At 17 DAI, the total root length, surface area and volume did not differ between NO_3^- treatments (Figure S1). Similar trends were observed for the length, surface area and volume of axial roots and lateral roots.

Tissue N

Independent of external NO_3^-, seed N reserves depleted by 8 DAI, with the majority depleting 5–8 DAI (Figure 2A). Shoot N% was high initially (8%) across both NO_3^- treatments, but rapidly diluted to less than 4% by 9 DAI, and stabilizing by 13 DAI (Figure 2B). Unlike

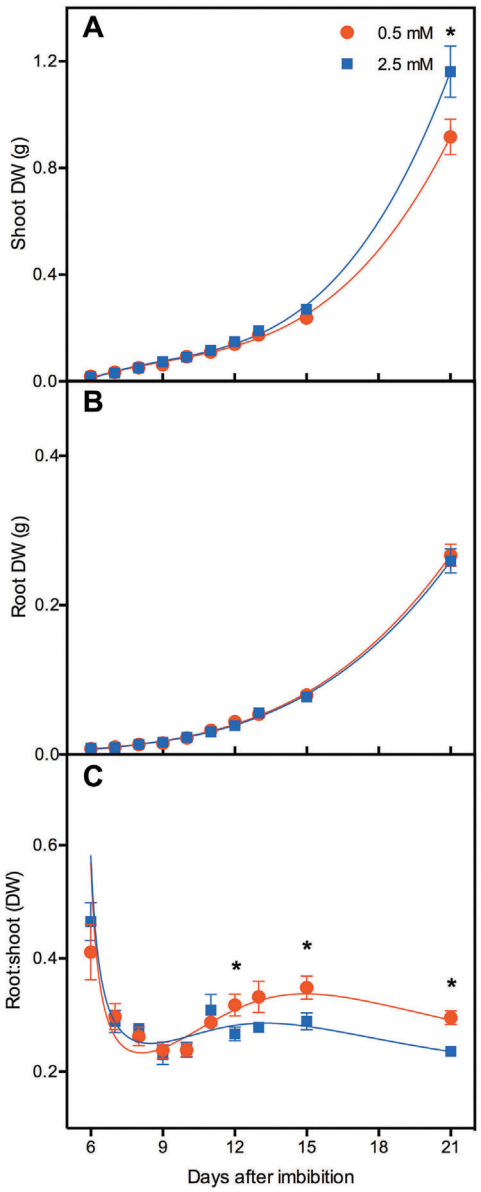

Figure 1. Growth parameters of *Zea mays* var. B73
Plants were grown in 0.5 mM (red circles) or 2.5 mM (blue squares) NO_3^-. **(A)** Shoot dry weight (DW), **(B)** root DW, and **(C)** root:shoot were measured until 21 d after imbibition. Cubic polynomial functions were fitted to tissue DWs. Values generated from cubic functions were plotted along with root:shoot (solid lines). Values are means ± *SEM* ($n = 8$). *Points significantly different between the two growth conditions ($P < 0.05$).

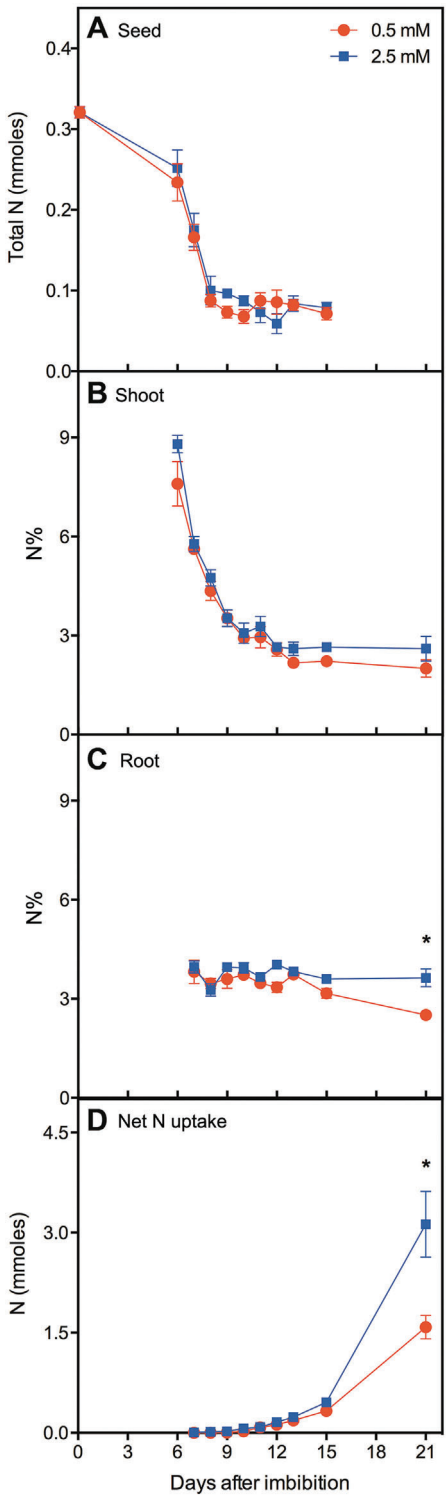

Figure 2. Nitrogen content in *Zea mays* var. B73 tissue
Plants were grown in 0.5 mM (red circles) or 2.5 mM (blue squares) NO_3^- and **(A)** total seed N, N% in **(B)** shoot, and **(C)** root tissue was measured from dried samples. **(D)** Net N uptake values were calculated as described in materials and methods. Values are means ± *SEM* ($n = 4$). *Points significantly different between the two growth conditions ($P < 0.05$).

the shoots, root N% was maintained at 4% throughout all sampling days across the 2.5 mM NO_3^- treatment, whereas those in the 0.5 mM treatment decreased 15–21 DAI (Figure 2C).

To examine how net N uptake was affected by external NO_3^- supply, the net N uptake was calculated

per plant, taking the seed derived N into account. Net N uptake per plant remained at baseline until 9 DAI, where it then began to steadily increase. By 21 DAI, net N uptake was influenced by NO_3^- supply, with seedlings in 0.5 mM NO_3^- capturing 50% less N than those in the 2.5 mM treatment (Figure 2D).

Tissue NO_3^- concentrations

In the 0.5 mM NO_3^- treatment, shoot NO_3^- concentrations remained stable through to the final sampling day (Figure 3A). In 2.5 mM NO_3^-, shoot NO_3^- concentrations matched those in 0.5 mM until the final sampling day, when concentrations were higher in 2.5 mM NO_3^- than in the 0.5 mM treatment. Across both NO_3^- treatments, root NO_3^- concentrations generally decreased until 11 DAI (Figure 3B). However, root NO_3^- concentrations were generally lower in seedlings grown in 0.5 mM NO_3^-, compared to those grown in the 2.5 mM treatment.

Free amino acids

In both NO_3^- treatments, concentrations of total free amino acids in shoots (Figure 3C) and roots (Figure 3D) decreased rapidly until 8 DAI, and was similarly observed for concentrations of most individual free amino acids (Figure S2). Of the individual free amino acids that were present in high concentrations, asparagine was initially the highest in both shoot and root tissue. In seedlings grown in 0.5 mM NO_3^-, concentrations of shoot glycine, glutamine and alanine dropped until 8 DAI, then remained steady until the final sampling day, whereas concentrations in 2.5 mM NO_3^- increased 15–21 DAI. Concentrations of root glycine, glutamine and alanine shared a similar trend with root asparagine and did not differ between NO_3^- treatments across sampling days. Glutamate concentrations in shoot and root tissue dropped until 8 DAI in both NO_3^- treatments, then remained steady; this was not, however, to the same magnitude as the amino acids described above.

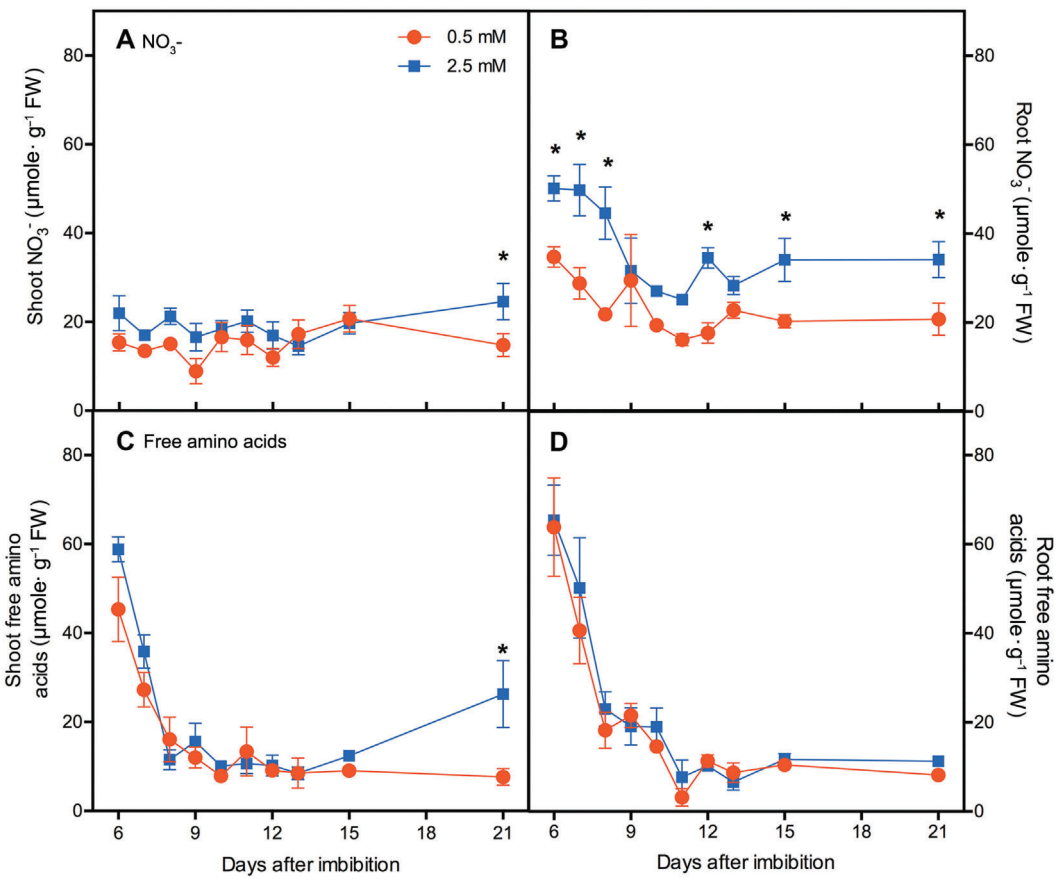

Figure 3. NO_3^- and free amino acid concentrations

Concentrations of **(A)** shoot NO_3^-, **(B)** root NO_3^-, and total free amino acid concentrations in the **(C)** shoot and **(D)** root of fresh *Zea mays* var. B73. Plants were grown in 0.5 mM (red circles) or 2.5 mM (blue squares) NO_3^-. Values are means ± *SEM* ($n = 4$). *Points significantly different between the two growth conditions ($P < 0.05$).

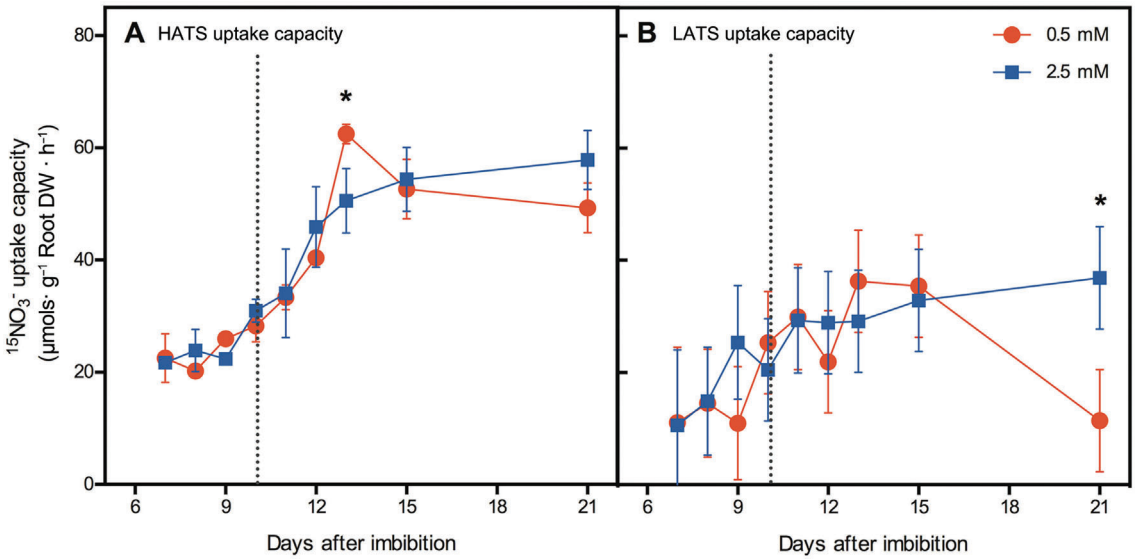

Figure 4. Root NO_3^- uptake capacity in *Zea mays* var. B73 tissue
(A) HATS and **(B)** calculated LATS NO_3^- uptake capacity of *Zea mays* var. B73 grown in 0.5 mM (red circles) or 2.5 mM (blue squares) NO_3^-. HATS values are means ± *SEM* ($n = 4$), whereas those of LATS are calculated means ± *SED*. Dotted line at 8 DAI represents the time-point when free amino acids concentrations began to stabilize. *Points significantly different between the two growth conditions (HATS $P < 0.05$; LATS $\alpha = 0.05$).

Root NO_3^- uptake capacity

In 2.5 mM NO_3^-, HATS NO_3^- uptake capacity increased rapidly from 10 DAI, then plateaued from 15 DAI at levels three times higher than baseline activity (Figure 4A). This was similarly observed within seedlings grown in 0.5 mM NO_3^-; however, HATS NO_3^- uptake capacity peaked 13 DAI, at levels higher than those in the 2.5 mM treatment, before stabilizing at 15 DAI. Similar trends were observed for HATS NO_3^- uptake capacity relative to root surface area for both NO_3^- treatments (Figure S3). Mean LATS NO_3^- uptake capacity began increasing after 8 DAI (Figure 4B), reaching maximum capacity, double compared to baseline activity, at 12 DAI regardless of NO_3^- supply, with peak NO_3^- uptake rates being lower than those of the HATS. In 0.5 mM NO_3^-, LATS uptake capacity decreased back to baseline activity 15–21 DAI, to half the capacity of the seedlings grown in the 2.5 mM treatment.

Root NO_3^- transporter (NRT) gene expression

Transcript levels of genes encoding putative high-affinity NO_3^- transporters ZmNRT2.1 (Figure 5A), ZmNRT2.2 (Figure 5B), and ZmNRT3.1A (Figure 5C) began increasing 10 DAI in both NO_3^- treatments. Transcript levels of *ZmNRT2.1*, *ZmNRT2.2* and *ZmNRT3.1A* increased until 15 DAI, after which transcript levels stabilized. *ZmNRT2.2* transcript levels were lower in seedlings grown in 0.5 mM NO_3^-, compared to those in the 2.5 mM treatment, with treatment differences emerging at 21 DAI. Similar to *ZmNRT2.1*, transcript levels of *ZmNRT3.1A* increased from 10 DAI and plateaued from 15 DAI, regardless of NO_3^- supply. *ZmNRT2.5* transcript levels remained close to zero until 15 DAI, in both NO_3^- treatments. Subsequently, transcript levels in 0.5 mM NO_3^- grown seedlings increased to levels three times higher than those in the 2.5 mM treatment (Figure 5D).

Transcript levels of *ZmNPF6.3A* were highest during early growth (6 DAI) and generally decreased until 21 DAI in seedlings grown in the 0.5 mM NO_3^- treatment (Figure 5E). Conversely, *ZmNPF6.3A* transcript levels in seedlings grown in 2.5 mM NO_3^- were lowest 6–9 DAI, then began increasing from 10 DAI, peaking at 15 DAI before decreasing from 15–21 DAI. Transcript levels of *ZmNPF6.3B* in seedlings grown in 0.5 mM NO_3^- remained steady across sampling days, whereas those in the 2.5 mM treatment increased from 10 DAI and generally remained higher than those in 0.5 mM NO_3^- (Figure 5F). Transcript levels of *ZmNPF7.3A* decreased by more than half 8–9 DAI across both NO_3^- treatments, and then remained steady through the remaining sampling days (Figure 5G).

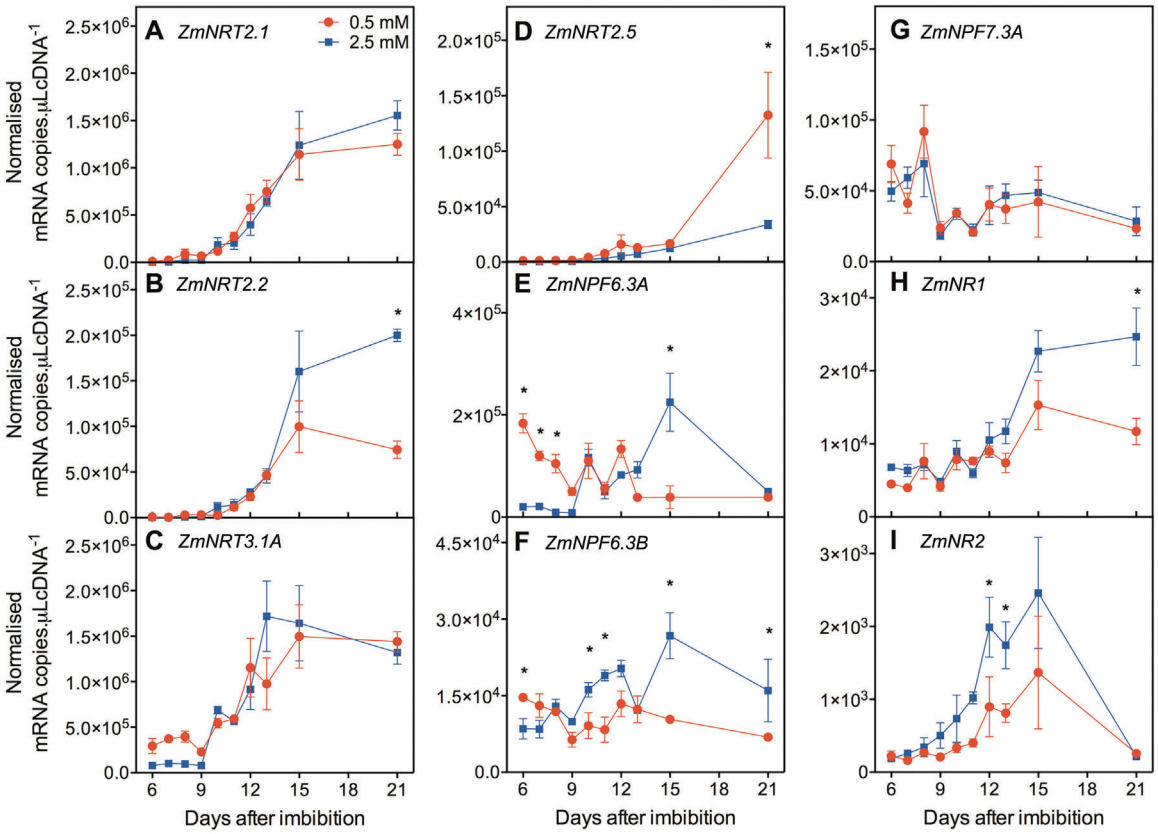

Figure 5. mRNA transcripts levels in *Zea mays* var. B73 roots
Transcript levels of **(A)** *ZmNRT2.1*, **(B)** *ZmNRT2.2*, **(C)** *ZmNRT3.1A*, **(D)** *ZmNRT2.5* **(E)** *ZmNPF6.3A* **(F)** *ZmNPF6.3B*, **(G)** *ZmNRT7.3A, and NADH:NR* genes, **(H)** *ZmNR1* and **(I)** *ZmNR2* in maize roots (*Zea mays* var. B73). Plants were grown in 0.5 mM (red circles) or 2.5 mM (blue squares) NO_3^-. Each data point is normalized to control genes as described in materials and methods. Values are means ± *SEM* ($n = 4$). *Points significantly different between two growth conditions ($P < 0.05$).

Root nitrate reductase (NR) gene expression

ZmNR1 transcript levels were similar in both NO_3^- treatments and slowly increased from 13 DAI (Figure 5H). In seedlings grown in 0.5 mM NO_3^-, *ZmNR1* transcripts reached maximum levels 15 DAI, whilst those in the 2.5 mM treatment increased to levels twice those of seedlings grown in 0.5 mM NO_3^- 21 DAI, similar to trends of *ZmNRT2.2* transcript levels.

ZmNR2 transcript levels followed a trend that was different from *ZmNR1*. In seedlings grown in 0.5 mM NO_3^-, *ZmNR2* transcript levels began increasing 10 DAI, reaching peak levels at 15 DAI, before decreasing to reach baseline at 21 DAI (Figure 5I). A similar pattern was observed in seedlings grown in 2.5 mM NO_3^-; however, *ZmNR2* transcript levels began increasing one day earlier, at 9 DAI, and reaching levels higher than those of the 0.5 mM treatment 12–13 DAI, before returning to baseline level 15–21 DAI.

DISCUSSION

This study exploited the seedlings transition from seed N use to external N capture to investigate the physiological processes, in particular, those within the root, to better understand how NO_3^- uptake upregulates to meet plant N demand. During early growth, root:shoot, shoot N% and concentrations of shoot and root free amino acids decreased rapidly until 8 DAI, independent of external NO_3^- supply. This is in agreement with Srivastava et al. (1976), and shows that external NO_3^- supply had little effect on maize seedling N content whilst growth was being supported by the seed. Although the decreasing shoot N% is due to dilution as a consequence of shoot emergence, it is likely that free amino acid concentrations decrease rapidly due to a combination of dilution and incorporation into newly-synthesized proteins.

Following seed N exhaustion and the dramatic decrease in root:shoot and free amino acid concentrations, root NO_3^- uptake capacity increased, reaching maximum rates by 12–13 DAI, when shoot N% stabilised. The rise in HATS NO_3^- uptake capacity corresponded with *ZmNRT2.1* and *ZmNRT2.2* transcript levels, suggesting that these NRTs facilitate root HATS NO_3^- uptake in maize. Numerous studies have characterized root NO_3^- uptake using <7 d old maize seedlings (Neyra and Hageman 1975; Colmer and Bloom 1998; Taylor and Bloom 1998). The results obtained from these former studies should be interpreted in light of the observation here that transcription of NO_3^- inducible *NRT2* genes and NO_3^- uptake capacity itself had not risen substantially in the developing seedling by this time. The rise in NO_3^- uptake capacity and levels of *ZmNRT2.1* and *ZmNRT2.2* transcripts corresponded with a rise in the level of *ZmNRT3.1A* transcripts, strengthening the possible association of ZmNRT3.1A with NO_3^- uptake in maize, as shown in *Arabidopsis* (Okamoto et al. 2006; Wirth et al. 2007). This suggests that differences in HATS activity profiles, according to the NO_3^- treatment, may also be related to reduced *ZmNRT3.1A* transcription, given the role of NRT3.1 to regulate NRT2 NO_3^- transport activity (Okamoto et al. 2006; Yan et al. 2011; Kotur et al. 2012). Prior to the increase in root NO_3^- capture, there was an abundance of root *ZmNPF6.3* transcripts. We hypothesize that this may provide base-level root NO_3^- uptake whilst N demand is low; then, as seedling N demand rises and is not met by NPF-mediated NO_3^- uptake, *NRT2* transcription and HATS uptake is upregulated.

Given transcript levels of *ZmNRT2.1*, *ZmNRT2.2*, *ZmNRT3.1A*, *ZmNR1*, *ZmNR2* and NO_3^- uptake capacity all increase shortly after free amino acid concentrations decrease, it is likely that this may be the physiological cue triggering the upregulation of the NO_3^- uptake system. This is supported by earlier studies which showed that NR activity rises as the products of seed protein hydrolysis deplete (Sivasankar and Oaks 1995), and those suggesting that the repression of *NRT2* transcription and root NO_3^- uptake following exogenous amino acids application may be the result of free amino acid accumulation in tissues, in particular glutamine (Zhuo et al. 1999; Vidmar et al. 2000; Nazoa et al. 2003). Indeed, in this study, root NO_3^- concentrations also decreased prior to the increase in NO_3^- uptake capacity; however, it is not believed that the observed decrease contributes to the physiological cue, as treatment differences in root NO_3^- concentrations were not reflected in the NO_3^- uptake capacity. Additionally, shoot NO_3^- concentrations remained constant across the transition from seed N use to external N capture, which excludes the involvement of shoot NO_3^- concentrations to the cue.

Based on a study investigating N uptake across the maize lifecycle, Garnett et al. (2013) proposed that maize increases HATS NO_3^- uptake capacity, to meet N demand. The first response to meet N demand is to utilize any latent NO_3^- uptake capacity (existing root NO_3^- uptake transporters under post-transcriptional and/or post-translational regulation), followed by an increase in *ZmNRT2.1*, *ZmNRT2.2* transcription. However, in this case, this is the first time young seedlings have increased HATS NO_3^- uptake capacity to meet demand, thus not possessing any latent NO_3^- uptake capacity to utilize. Consequently, insufficient N was captured by roots to maintain maximal shoot growth rate, reflected in decreased shoot growth and increased root:shoot in low N, relative to sufficient N. Further, the observation that NO_3^- treatment differences in root:shoot emerged 12 DAI highlights how early N limitation can impact growth and development in the maize lifecycle.

HATS NO_3^- uptake capacity peaked at 13 DAI in 0.5 mM NO_3^- grown plants, at levels exceeding those in the 2.5 mM treatment, then began to decrease. We speculate this reflects that plants grown in 0.5 mM NO_3^- required greater NO_3^- uptake capacity to meet their N demand, and transcript levels of putative NO_3^- transporters involved in root NO_3^- uptake did not differ because release of post-translational control of uptake capacity facilitating N demand to be met. In this case, the post-translational control may possibly occur by changing the way ZmNRT2.1 and ZmNRT3.1A is assembled in the plasma membrane (Wirth et al. 2007), potentially influencing HATS activity. Similarly, there is evidence of post-translational control after 13 DAI, in that the HATS activity reduces whilst transcript levels of *ZmNRT2.1* and *ZmNRT2.2* continue to increase 13–15 DAI.

ZmNRT2.5 was the only *NRT2* that was upregulated in low N, supporting its possible involvement in responses to low N limitation (Garnett et al. 2013, Lezhneva et al. 2014); however, the transcript profile of *ZmNRT2.5* does not correspond with NO_3^- uptake capacity. In *Arabidopsis* roots, the expression of *AtNRT2.5* is localized to

the epidermis and cortex of roots at the root hair zone and facilitates HATS NO_3^- uptake in N-starved plants (Kotur et al. 2012; Lezhneva et al. 2014). Conversely, the rice NRT2.5 orthologue is mainly expressed in xylem parenchyma cells of the root stele and plays a key role in root to shoot NO_3^- transport in low NO_3^-, suggesting that it may be the inducible HATS component involved in NO_3^- loading into the xylem (Tang et al. 2012). Given the discrepancy between *Arabidopsis* and cereals in terms of the localization and proposed function of NRT2.5, further investigation is required to clarify the role of this protein, at least in cereals.

Transcript profiles of *ZmNPF6.3A*, *ZmNPF6.3B* differ to root NO_3^- uptake capacity. *ZmNPF6.3A* transcript levels in plants grown in 2.5 mM NO_3^- are greater than those in 0.5 mM NO_3^- at 15 DAI, whilst for *ZmNPF6.3B*, these NO_3^- treatment difference exist 10–21 DAI. NPF6.3 may be facilitating root to shoot translocation here, as described in *Arabidopsis* by Léran et al. (2013). With greater NO_3^- concentrations in root tissue in 2.5 mM NO_3^-, relative to 0.5 mM, a greater requirement for root to shoot NO_3^- translocation exists, to facilitate assimilation. However, as the role of NPF6.3 remains convoluted (Glass and Kotur 2013), further evidence is required to assume its role in both *Arabidopsis* and cereals.

Apart from NO_3^- in the roots, there was little difference in free amino acid or NO_3^- tissue concentrations between NO_3^- treatments. The root NO_3^- concentration being higher in the 2.5 mM NO_3^- treatment, but not the shoots, is thought to reflect that higher NO_3^- availability, but suggest root to shoot transport of NO_3^- is limiting and supports the hypothesis regarding NPF6.3 above. This hypothesis supports that both the shoot-free amino acid and NO_3^-concentrations were higher in the 2.5 mM NO_3^- treatment only at 21 DAI, suggesting that it was only at that time that supply of N to the shoot was meeting the demand cause by growth.

Despite the differences between NO_3^- treatments in net N uptake and growth, the processes leading to and involved in the upregulation of the NO_3^- uptake system were found to be similar. Seed N content and free amino acid concentrations decreased rapidly until 8 DAI, followed by an increase in root NO_3^- uptake capacity, corresponding with a rise in *ZmNRT2.1*, *ZmNRT2.2*, *ZmNRT3.1A* transcript levels. Then, as seedlings developed and N demand increased, low N supply had an impact on growth, as reflected in an increase in root:shoot, up to values beyond those for seedlings in sufficient N. This observation may be explained on the basis that during early growth, low N supply may satisfy

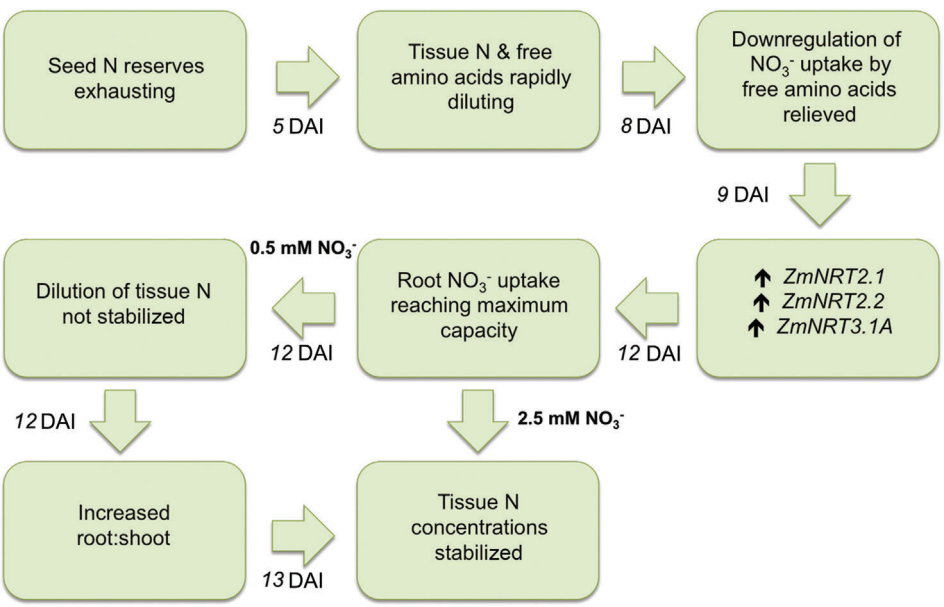

Figure 6. Proposed model
Proposed model outlining the way that maize (*Zea mays* L.) seedlings manage the transition from seed N use to external NO_3^- capture in order to maintain plant N status.

the N demand of seedlings, whereas later, N demand may exceed low supply, suggesting that small differences in N uptake and growth early in growth become magnified over time as a consequence of increasing N demand.

Given the order of the physiological processes involved in NO_3^- uptake and assimilation observed, a model is proposed that outlines the key processes managing the transition from seed N use to external N capture (Figure 6). It is believed that this model captures the way in which seedlings manage this transition, thereby maintaining control of plant N status during early vegetative growth, and further describes how this transition can be influenced by NO_3^- supply. This model highlights how rapidly the plant's system responds to N supply and demand, even with steady external N supply, which is important when investigating the regulation of these plant processes. Here, *ZmNRT2.1*, *ZmNRT2.2* and *ZmNRT3.1A* transcription increased 9–15 DAI, following the decrease in free amino acid concentrations and resulted in a tripling in HATS activity, before reaching maximum capacity. Further investigation into the global transcriptional profiles at time points within this period may lead to the identification of genes following similar/opposite expression patterns to these HATS associated genes, as well as genes that may be upstream of, and, regulating the NRTs. Execution of such an investigation with high-temporal resolution could contribute to systems biology approaches to elucidating the regulation of N uptake, by mapping components involved in N-signalling and N uptake, and the order they may lie within the hierarchy of the signalling network (Krouk et al. 2010; Gutiérrez 2012). Among 0.5 mM NO_3^- grown seedlings, changes to root:shoot, relative to those in the 2.5 mM treatment, occurred 12 DAI, when root NO_3^- uptake capacity almost reached maximum rates. Although this highlights how early in development N limitation impacts growth; this period offers the opportunity to use global transcription analysis on root and shoot tissue to identify potential regulators of biomass allocation.

The development of such a model in seedlings is important for future research efforts, as it relates well to processes in older maize plants that increase root NO_3^- uptake capacity to meet N demand (Garnett et al. 2013). This means that studies investigating the upregulation of NO_3^- uptake capacity in steady-state N conditions, rather than N-starvation, can be explored in cereal crops using young seedlings that are less than 2 weeks old, rather than growing them for longer periods of time, which consumes more time, space and resources. Although the proposed model is generally applicable to maize, the corresponding DAI of transitional steps are likely specific to our particular experiment and may change with environment and plant species. The model may also be applicable to other stages of the plant lifecycle during which root NO_3^- uptake capacity increases to meet demand, keeping in mind that any latent NO_3^- uptake capacity will preferentially be utilized before *ZmNRT2.1*, *ZmNRT2.2*, *ZmNRT3.1A* transcription. It is worth investigating how the processes within this study are influenced by seed N content, not only using seeds with differing initial N content, but also excising seed at different time-points during seeding establishment, in order to determine how the quantity of maternal N source influences the transition. Wider ranges of external N supply could also be used to further validate the model, as well as different maize varieties. By understanding how maize upregulates root NO_3^- uptake, we identify potential controls/cues (free amino acid concentrations, HATS activity and the associated *NRTs*). It is anticipated that such controls/cues can become targets for manipulation, in order to increase root NO_3^- (e.g., greater free amino acid to protein conversion to lower total free amino acid concentration).

MATERIALS AND METHODS

Plant growth

Maize seeds (*Zea mays* L. var. B73) of similar size were imbibed in aerated RO-H_2O for 24 h at room temperature, after which they were transferred onto filter paper moistened with 0.5 mM $CaCl_2$ (3 d, 26 °C, dark). Germinating seedlings were then transferred to one of eight 120 L ebb and flow hydroponic systems, with a complete fill/drain cycle of 30 min (four separate systems for each NO_3^- treatment). Individual seedlings were grown on mesh collars within tubes (300 × 50 mm). This allowed the roots to remain separate from adjacent seedlings while allowing free access to solution. The hydroponic system was situated in a controlled environment room with a day/night cycle of 14 h at 26 °C/10 h at 20 °C, with a flux density at canopy

level of 650 μmol m^{-2} s^{-1} and relative humidity of 60%. The nutrient solution was a modified Johnson's solution (Johnson et al. 1957) containing (in mM): 0.5 NO_3^- N, 0.8 K, 0.1 Ca, 0.5 Mg, 1 S and 0.5 P for the 0.5 mM NO_3^- treatment, and 2.5 NO_3^- N, 1.8 K, 0.6 Ca, 0.5 Mg, 0.5 S, 0.5 P for the 2.5 mM NO_3^- treatment. The choice of NO_3^- concentrations was based on those used by Garnett et al. (2013), who suggested that 0.5 mM was the threshold concentration eliciting a major response in the maize NO_3^- uptake system. Both treatment solutions also contained (in μmol/L): 2 Mn, 2 Zn, 25 B, 0.5 Cu, 0.5 Mo, and 100 Fe (as FeEDTA and ethylendiamine-*N*, *N*'-bis(2-hydroxyphenylacetic acid) (FeEDDHA)). Iron was supplemented twice weekly with the addition of $Fe(NH_4)_2(SO_4)_2.6H_2O$ (8 mg L^{-1}) to avoid deficiency (Cramer et al. 1994). Solutions were maintained between 19–21 °C using a refrigerated chiller. Solution pH was maintained between 5.8–6.0 and nutrient solutions were changed every 7 d. Concentrations of NO_3^- were monitored using a NO_3^- electrode (TPS, Springwood, Qld, Australia) and maintained at the target concentration ±5%. Other nutrients were monitored using an inductively coupled plasma optical emission spectrometer (ICP-OES: ARL 3580 B, ARL, Lausanne, Switzerland) and showed limited depletion between solution changes.

Measurement of root traits

On sampling days, maize seedling roots were separated from the remainder of the plant, blotted, and weighed to obtain fresh weights (FW). Seedling roots were then scanned as a digital image (Epson Expression 10000XL), and root parameters (length, surface area, volume, average diameter and root tip number) were determined from scanned root images using WinRHIZO Pro root image analysis software (V.2005b, Regent Instruments, Quebec, Canada). Axial roots comprise both primary and seminal roots, whereas lateral roots are defined as the roots developing from axial roots (Figure S4). Lateral roots were differentiated from the axial roots with WinRHIZO, using a distinguishing diameter of 0.677 mm (verified for both NO_3^- treatments). The number of axial roots was counted manually from digital images, whereas the lateral root number was calculated by subtracting the number of axial roots from the total number of root tips. Although the number of tips included the points where the root was cut, this was negligible (<2%). The average lateral and axial root length was calculated by dividing the total length of the respective root type by the total number of that root type. Lateral root density was calculated by dividing the total number of root tips by total axial root length.

Determination of tissue N and cumulative net N uptake

To determine total tissue N content, sampled plants were blotted and the roots, shoots, and seed were separated and dried (5 d, 60 °C), weighed and ground to a fine powder (Clarkson et al. 1996). The total amount of N within each sample was determined using an isotope mass spectrometer (Sercon, Crewe, Cheshire, UK). Cumulative net N uptake, taking into account the amount of seed-derived N within the plant, was calculated using the formula below, where T_n denotes the day of sampling and T_o is the time point before imbibition. Nitrogen in shoots (ShN) and roots (RN) were added to derive total plant N. Subsequently, the cumulative amount of seed N (SN) calculated to be translocated into the seedling (T_o–T_n) was subtracted from total plant N:

$$\text{Net N uptake}_{Tn} = (\text{ShN}_{Tn} + \text{RN}_{Tn}) - \text{SN}_{To-Tn}$$

Amino acid analysis

Concentrations of free amino acids in root and shoot tissue were determined using liquid chromatography electrospray ionization-mass spectrometry as described by Boughton et al. (2011).

Tissue NO_3^- determination

To extract NO_3^- from plant tissue, 20 mg of homogenous finely ground frozen plant tissue was added to 1 mL MQ-H_2O and boiled in a water bath (20 min, 95–100 °C). The boiled samples were then cooled and centrifuged (12,000 *g*, 15 min). For analysis, 50 μL supernatant was added to 200 μL 5% w/v salicylic acid in H_2SO_4 and incubated (20 min, RT). Then, 125 μL of the mixture containing the sample and 5% w/v salicylic acid in H_2SO_4 was added to NaOH (2.375 mL, 2 N) and incubated (20 min, RT). Processed samples were then loaded into 96-flat well plates (200 μL/well) (Greiner Bio-One, Vic, Australia), read at an absorbance of 410 nm (POLARstar Optima, BMG Labtech, Germany), and compared against KNO_3 standards.

NO_3^- uptake capacity measurement

On sampling days, between 11:00 and 13:00 h, plants were transferred to nutrient solutions that matched the growth solutions within the same controlled environment conditions. Roots were then rinsed for 5 min with the same nutrient solution, but with either 100 μM or 1,000 μM NO_3^-, followed by 10 min of exposure to the same solution, but with ^{15}N-labelled NO_3^- (^{15}N 10%). The concentration of 100 μM NO_3^- was used because it is close to saturation of the HATS and 1,000 μM would include activity of both, HATS and some LATS (Siddiqi et al. 1990; Kronzucker et al. 1995a; Crawford and Glass 1998). At the end of the ^{15}N incubation flux period, roots were rinsed for 2 min in matching, but unlabelled, solutions. Two identical solutions were used for this rinse to allow an initial 5 s rinse to remove labeled solution adhering to the root surface. The flux timing was based on that used by Kronzucker et al. (1995b) and chosen to minimize ^{15}N efflux back into the solution. Roots were then blotted and separated from shoots, dried (5 d, 60 °C), weighed and ground to a fine powder (Clarkson et al. 1996). The amounts of ^{15}N in the plant samples were determined using an isotope mass spectrometer (Sercon, Crewe, Cheshire, UK). Nitrate uptake capacity was calculated on the basis of ^{15}N content in the plant. Mean LATS uptake capacity for a given time-point was calculated by subtracting the mean 100 μM NO_3^- uptake capacity value from that of 1,000 μM NO_3^- uptake capacity, at the same time-point and NO_3^- treatment (Okamoto et al. 2003). Error bars for calculated LATS NO_3^- uptake capacity plots (1,000 μM − 100 μM) represent the standard error of difference (SED) between NO_3^- treatments (0.5 mM and 2.5 mM NO_3^-), which was calculated using the equation below:

$$\mathrm{SED}_{1000\ \mu M-100\ \mu M} = \sqrt{\sigma^2(1000\ \mu M) + \sigma^2(100\ \mu M)}$$

σ represents the standard error of a mean (SEM) of 100 μM or 1,000 μM NO_3^- uptake capacity measurement, and is calculated using the below equation:

$$\sigma = \frac{\mathrm{SED}(0.5\ \mathrm{mM\ vs.}\ 2.5\ \mathrm{mM})}{\sqrt{2}}$$

HATS NO_3^- uptake capacity was also calculated relative to the root surface area. Root surface area (cm^2) of dried roots exposed to the ^{15}N flux was calculated from the original FWs using the linear relationship between root FW and surface area (Figure S5). Individual regressions were determined for each NO_3^- treatment.

Real-time quantitative PCR (Q-PCR)

On sampling days, root material was harvested between 11:00 and 13:00 h (5–7 h after start of light period). Whole roots were excised and snap frozen in liquid N_2 and stored at −80 °C. Homogenous finely-ground frozen root tissue (100 mg) was added to 1 mL TRIzol-like reagent, containing 38% v/v phenol (equilibrated pH 4.3, Sigma-Aldrich, Australia), 11.8% w/v guanidine thiocyanate, 7.6% w/v ammonium thiocyanate, 3.3% v/v sodium acetate (3 M, pH 5), 5% v/v glycerol, and made up to 100% v/v with MQ-H_2O. Extraction of RNA was performed using the method of Chomczynski (1993). Extracted RNA was DNase treated (Ambion, USA) according to the manufacturer's instructions. The integrity of the RNA was confirmed by 1.2% w/v agarose gel electrophoresis. cDNA synthesis was performed with 1 μg of DNase treated total RNA, using SuperScript III reverse transcriptase (Invitrogen, Carlsbad, CA, USA), according to the manufacturer's instructions. Q-PCR was carried out as outlined in Burton et al. (2008) and Garnett et al. (2013). Four control genes (*ZmGaPDh*, *ZmActin*, *ZmTubulin* and *ZmElF1*) were used to calculate the normalisation factor. Primer sequences were the same as those used by Garnett et al. (2013), except for *ZmNPF6.3B* (GRMZM2G161459: forward primer: 5'-GTCATCAGCGCCATCAACCT, reverse primer: 5'- ACGG-CAATAGACTCCTCGTC); and two *NADH:NR* genes, *NR1* (GRMZM2G568636: forward primer: 5'- GAGGACCA-CACGGAGATG, reverse primer: 5'- CCAACGCTGTAC TTCCAC) and *NR2* (GRMZM2G428027: forward primer: 5'- GCTTTGGCTAACGAATGT C, reverse primer: 5'-GCTCGCTACTATTACAACAAG) (Long et al. 1992).

Statistical analyses

Seedlings were grown and selected randomly from four separate hydroponic systems corresponding to NO_3^- treatment, which constituted blocks. There was no significant difference between blocks. Statistical analysis for calculated LATS NO_3^- uptake capacity was carried out using a student t-test for two independent means. All other statistical analyses within this study were carried out using two-way analysis of variance (ANOVA).

ACKNOWLEDGEMENTS

We thank Hanne Thompson, Yuan Li, Nenah Mackenzie, Priyanka Reddy and Chia Ng for the technical assistance provided for this study. We also thank Metabolomics Australia, School of BioSciences, The University of Melbourne, for sample preparation and amino acid analysis. Ute Roessner and Berin Boughton are also grateful to Victorian Node of Metabolomics Australia, which is funded through Bioplatforms Australia Pty Ltd, a National Collaborative Research Infrastructure Strategy, 5.1 Biomolecular Platforms and informatics investment, and co-investment from the Victorian State Government and The University of Melbourne. This project was supported by the Australian Centre for Plant Functional Genomics, the Australian Research Council (LP130101055), DuPont Pioneer and the Grains Research and Development Corporation (GRS10437).

AUTHOR CONTRIBUTIONS

K.S., D.P., T.G. designed and conceived the research. K.-S., L.H., J.G. performed the experiments; B.B. and U.R. performed the quantification of the free amino acids; M.T., S.H. contributed to the discussion and editing; K.S., D.P., T.G. wrote the manuscript.

REFERENCES

Boughton BA, Callahan DL, Silva C, Bowne J, Nahid A, Rupasinghe T, Tull DL, McConville MJ, Bacic A, Roessner U (2011) Comprehensive profiling and quantitation of amine group containing metabolites. **Anal Chem** 83: 7523–7530

Burton RA, Jobling SA, Harvey AJ, Shirley NJ, Mather DE, Bacic A, Fincher GB (2008) The genetics and transcriptional profiles of the cellulose synthase-like HvCslF gene family in barley. **Plant Physiol** 146: 1821–1833

Chapin FSIII, Bloom AJ, Field CB, Waring RH (1987) Plant responses to multiple environmental factors. **BioScience** 37: 49–57

Chomczynski P (1993) A reagent for the single-step simultaneous isolation of RNA, DNA and proteins from cell and tissue samples. **Biotechniques** 15: 532–534

Clarkson DT, Gojon A, Saker LR, Wiersema PK, Purves JV, Tillard P, Arnold GM, Paans AJ, Vaalburg W, Stulen I (1996) Nitrate and ammonium influxes in soybean (*Glycine max*) roots -direct comparison of N-13 and N-15 tracing. **Plant Cell Environ** 19: 859–868

Colmer TD, Bloom AJ (1998) A comparison of NH_4^+ and NO_3^- net fluxes along roots of rice and maize. **Plant Cell Environ** 21: 240–246

Cramer GR, Alberico GJ, Schmidt C (1994) Leaf expansion limits dry-matter accumulation of salt-stressed maize. **Aust J Plant Physiol** 21: 663–674

Crawford NM, Glass ADM (1998) Molecular and physiological aspects of nitrate uptake in plants. **Trends Plant Sci** 3: 389–395

Forde BG (2002) Local and long-range signaling pathways regulating plant responses to nitrate. **Annu Rev Plant Biol** 53: 203–224

Garnett T, Conn V, Plett D, Conn S, Zanghellini J, Mackenzie N, Enju A, Francis K, Holtham L, Roessner U, Boughton B, Bacic A, Shirley N, Rafalski A, Dhugga K, Tester M, Kaiser BN (2013) The response of the maize nitrate transport system to nitrogen demand and supply across the lifecycle. **New Phytol** 198: 82–94

Glass ADM, Siddiqi MY (1995) Nitrogen absorption by plant roots. In: Srivastava HS, Singh RP, eds. *Nitrogen Nutrition in Higher Plants*. Associated Publishing Co, New Delhi, pp. 21–56

Glass AD, Kotur Z (2013) A reevaluation of the role of *Arabidopsis* NRT1.1 in high-affinity nitrate transport. **Plant Physiol** 163: 1103–1106

Glass ADM (2003) Nitrogen use efficiency of crop plants: Physiological constraints upon nitrogen absorption. **Crit Rev Plant Sci** 22: 453–470

Gutiérrez RA (2012) Systems biology for enhanced plant nitrogen nutrition. **Science** 336:1673–1675

Harvey B, Oaks A (1974) The hydrolysis of endosperm protein in *Zea mays*. **Plant Physiol** 53: 453–457

Heffer P (2013) *Assessment of Fertiliser Use by Crop at the Global Level 2010-2010/11*. International Fertiliser Industry, Paris, France

Ho CH, Lin SH, Hu HC, Tsay YF (2009) CHL1 functions as a nitrate sensor in plants. **Cell** 138: 1184–1194

Huang NC, Liu KH, Lo HJ, Tsay YF (1999) Cloning and functional characterization of an *Arabidopsis* nitrate transporter gene that encodes a constitutive component of low-affinity uptake. **Plant Cell** 11: 1381–1392

Ingestad T, Agren GI (1991) The influence of plant nutrition on biomass allocation. **Ecol Appl** 1: 168–174

Johnson CM, Stout PR, Brewer TC, Carlton AB (1957) Comparative chlorine requirements of different plant species. **Plant Soil** 8: 337–353

Kotur Z, Mackenzie N, Ramesh S, Tyerman SD, Kaiser BN, Glass ADM (2012) Nitrate transport capacity of the *Arabidopsis thaliana* NRT2 family members and their interactions with AtNAR2.1. **New Phytol** 194: 724–731

Kronzucker HJ, Glass ADM, Siddiqi MY (1995a) Nitrate induction in spruce: An approach using compartmental analysis. **Planta** 196: 683–690

Kronzucker HJ, Siddiqi MY, Glass ADM (1995b) Kinetics of NO_3^- influx in spruce. **Plant Physiol** 109: 319–326

Krouk G, Mirowski P, LeCun Y, Shasha D, Coruzzi G (2010) Predictive network modeling of the high-resolution dynamic plant transcriptome in response to nitrate. **Genome Biol** 11: R123

Léran S, Muños S, Brachet C, Tillard P, Gojon A, Lacombe B (2013) *Arabidopsis* NRT1. 1 is a bidirectional transporter involved in root-to-shoot nitrate translocation. **Mol plant** 6(6):1984–1987

Léran S, Varala K, Boyer JC, Chiurazzi M, Crawford N, Daniel-Vedele F, David L, Dickstein R, Fernandez E, Forde B, Gassmann W, Geiger D, Gojon A, Gong J, Halkier BA, Harris, JM, Hedrich R, Limami AM, Rentsch D, Seo M, Tsay Y, Zhang M, Coruzzi G, Lacombe B (2014) A unified nomenclature of NITRATE TRANSPORTER 1/PEPTIDE TRANSPORTER family members in plants. **Trends Plant Sci** 19: 5–9

Lezhneva L, Kiba T, Feria-Bourrellier AB, Lafouge F, Boutet-Mercey S, Zoufan P, Sakakibara H, Daniel-Vedele F, Krapp A (2014) The *Arabidopsis* nitrate transporter NRT2.5 plays a role in nitrate acquisition and remobilization in nitrogen-starved plants. **Plant J** 80: 230–241

Li W, Wang Y, Okamoto M, Crawford NM, Siddiqi MY, Glass ADM (2007) Dissection of the AtNRT2.1:AtNRT2.2 inducible high-affinity nitrate transporter gene cluster. **Plant Physiol** 143: 425–433

Long DM, Oaks A, Rothstein SJ (1992) Regulation of maize root nitrate reductase mRNA levels. **Physiol Plant** 85: 561–566

Malagoli P, Laine P, Le Deunff E, Rossato L, Ney B, Ourry A (2004) Modeling nitrogen uptake in oilseed rape cv Capitol during a growth cycle using influx kinetics of root nitrate transport systems and field experimental data. **Plant Physiol** 134: 388–400

Miller AJ, Fan XR, Orsel M, Smith SJ, Wells DM (2007) Nitrate transport and signalling. **J Exp Bot** 58: 2297–2306

Muller B, Touraine B (1992) Inhibition of NO_3^- uptake by various phloem-translocated amino acids in soybean seedlings. **J Exp Bot** 43: 617–623

Nazoa P, Vidmar JJ, Tranbarger TJ, Mouline K, Damiani I, Tillard P, Zhuo D, Glass AD, Touraine B (2003) Regulation of the nitrate transporter gene AtNRT2.1 in *Arabidopsis thaliana*: Responses to nitrate, amino acids and developmental stage. **Plant Mol Biol** 52: 689–703

Neyra CA, Hageman RH (1975) Nitrate uptake and induction of nitrate reductase in excised corn roots. **Plant Physiol** 56: 692–695

Okamoto M, Kumar A, Li W, Wang Y, Siddiqi MY, Crawford NM, Glass AD (2006) High-affinity nitrate transport in roots of *Arabidopsis* depends on expression of the NAR2-like gene AtNRT3.1. **Plant Physiol** 140: 1036–1046

Okamoto M, Vidmar JJ, Glass ADM (2003) Regulation of NRT1 and NRT2 gene families of *Arabidopsis thaliana*: Responses to nitrate provision. **Plant Cell Physiol** 44: 304–317

Parker JL, Newstead S (2014) Molecular basis of nitrate uptake by the plant nitrate transporter NRT1.1. **Nature** 507: 68–72

Peoples MB, Mosier AR, Freney JR (1995) Minimizing gaseous losses of nitrogen. In: Bacon PE, ed. *Nitrogen Fertilization in the Environment*. Marcel Dekker Inc, New York, pp. 565–602

Siddiqi MY, Glass ADM, Ruth TJ, Rufty TW (1990) Studies on the uptake of nitrate in barley. 1. Kinetics of $^{13}NO_3^-$ influx. **Plant Physiol** 93: 1426–1432

Sivasankar S, Oaks A (1995) Regulation of nitrate reductase during early seedling growth (A role for asparagine and glutamine). **Plant Physiol** 107: 1225–1231

Srivastava HS, Oaks A, Bakyta IL (1976) The effect of nitrate on early seedling growth in *Zea mays*. **Can J Bot** 54: 923–929

Sylvester-Bradley R, Kindred DR (2009) Analysing nitrogen responses of cereals to prioritize routes to the improvement of nitrogen use efficiency. **J Exp Bot** 60: 1939–1951

Tang Z, Fan X, Li Q, Feng H, Miller AJ, Shen Q, Xu G (2012) Knockdown of a rice stelar nitrate transporter alters long-distance translocation but not root influx. **Plant Physiol** 160: 2052–2063

Taylor A, Bloom A (1998) Ammonium, nitrate, and proton fluxes along the maize root. **Plant Cell Environ** 21: 1255–1263

Tischner R (2000) Nitrate uptake and reduction in higher and lower plants. **Plant Cell Environ** 23: 1005–1024

Vidmar JJ, Zhuo D, Siddiqi MY, Schjoerring JK, Touraine B, Glass ADM (2000) Regulation of high-affinity nitrate transporter genes and high-affinity nitrate influx by nitrogen pools in roots of barley. **Plant Physiol** 123: 307–318

Vitousek PM, Mooney HA, Lubchenco J, Melillo JM (1997) Human domination of Earth's ecosystems. **Science** 277: 494–499

Watt MP, Cresswell CF (1987) A comparison between the utilisation of storage protein and exogenous nitrate during seedling establishment in *Zea mays* L. **Plant Cell Environ** 10: 327–332

Wirth J, Chopin F, Santoni V, Viennois, G, Tillard P, Krapp A, Lejay L, Daniel-Vedele F, Gojon A (2007) Regulation of root nitrate uptake at the NRT2.1 protein level in *Arabidopsis thaliana*. **J Biol Chem** 282: 23541—23552

Wolt JD (1994) *Soil Solution Chemistry: Applications to Environmental Science and Agriculture*, John Wiley and Sons, New York

Yan M, Fan X, Feng H, Miller AJ, Shen Q, Xu G (2011) Rice OsNAR2.1 interacts with OsNRT2.1, OsNRT2.2 and OsNRT2.3a nitrate transporters to provide uptake over high and low concentration ranges. **Plant Cell Environ** 34: 1360–1372

Zhuo D, Okamoto M, Vidmar JJ, Glass ADM (1999) Regulation of a putative high-affinity nitrate transporter (*Nrt2;1At*) in roots of *Arabidopsis thaliana*. **Plant J** 17: 563–568

SUPPORTING INFORMATION

Additional Supporting Information may be found online in the supporting information tab for this article: http://onlinelibrary.wiley.com/doi/10.1111/jipb.12525/suppinfo

Figure S1. Root morphology

Root morphological parameters of *Zea mays* var. B73 seedlings grown in 0.5 mM (red circles) and 2.5 mM (blue squares) NO_3^-. Total **(A)** number, **(B)** length, **(C)** surface area, **(D)** volume, and **(E)** average length of axial roots, as well as total **(F)** number **(G)** density, **(H)** length, **(I)** surface area, **(J)** volume, and **(K)** average length of lateral roots were measured over a time course. Values are means ± *SEM* ($n = 6$). *Points significantly different between the two growth conditions ($P < 0.05$).

Figure S2. Individual free amino acid concentrations

Individual free amino acid concentrations in fresh shoot and root tissue of maize (*Zea mays* var. B73) grown in 0.5 mM (red circles) or 2.5 mM (blue squares) NO_3^-. Values are means ± *SEM* ($n = 4$). *Points significantly different between the two growth conditions ($P < 0.05$).

Figure S3. Maize (*Zea mays* var. B73) HATS NO_3^- uptake capacity, relative to root surface area

Seedlings were grown in 0.5 mM (red circles) or 2.5 mM (blue squares) NO_3^-. Values are means ± *SEM* ($n = 4$). *Points significantly different between the two growth conditions ($P < 0.05$). Dotted line at 8 DAI represents the time point at which concentrations of free amino acids began to stabilize.

Figure S4. Identification of lateral (LR) and axial roots (Ax) of maize seedlings (*Zea mays* L.)

Figure S5. Root fresh weight and surface area correlation

Correlations between root fresh weight and root surface area of maize (*Zea mays* var. B73) grown in **(A)** 0.5 mM NO_3^- and **(B)** 2.5 mM NO_3^-. All plants were sampled 7–17 DAI. Each data point represents a value for an individual plant and linear trend lines were fitted to determine each correlation.

Scan using WeChat with your smartphone to view JIPB online

Scan with iPhone or iPad to view JIPB online